

1 **Potential impacts of climate change on groundwater supplies to the Doñana wetland, Spain**

2 Carolina Guardiola-Albert¹ and Christopher R. Jackson²

3

4 1. Instituto Geológico y Minero de España, Calle Ríos Rosas 23, 28003 Madrid, España

5 2. British Geological Survey, Kingsley Dunham Centre, Keyworth, Nottingham, NG12 5GG, UK

6 Corresponding author: C Guardiola-Albert, c.guardiola@igme.es

7

8 **Keywords**

9 Anthropogenic effect, Groundwater/Surface water interactions, Modelling, Recharge

10 **Abstract**

11 Climate change impacts on natural recharge and groundwater-wetland dynamics were investigated
12 for the Almonte-Marismas aquifer, Spain, which supports the internationally important Doñana
13 wetland. Simulations were carried out using outputs from 13 global climate models to assess the
14 impacts of climate change. Reductions in flow from the aquifer to streams and springs flooding the
15 wetland, induced by changes in recharge according to different climate projections, were modelled.
16 The results project that the change in climate by the 2080s, under a medium-high greenhouse gas
17 emissions scenario, leads to a reduction in groundwater resources. The reduction in mean recharge
18 ranges from 14% to 57%. The simulations show that there is an impact on hydraulic head in terms
19 of the overall water table configuration with decreases in groundwater level ranging from 0 to 17 m.
20 Most simulations produce lower discharge rates from the aquifer to stream basins, with significant
21 reductions in the larger La Rocina (between -55% and -25%) and Marismas (between -68% and -
22 43%) catchments. Water flows from these two basins are critical to maintain aquatic life in the
23 wetland and riparian ecosystems. Modelled climate-induced reductions in total groundwater
24 discharge to the surface are generally larger than current groundwater abstraction rates. The results
25 highlight that effective strategies for groundwater resources management in response to future
26 climate change are imperative.

27 **1. Introduction**

28 Considered one of the most valuable wetlands in Europe, Spain's Doñana area, an intricate matrix
29 of marshlands and phreatic lagoons covering an area of 270 km², is a refuge for millions of
30 migratory birds and several endangered species. However, public and tourist water demands,
31 industrial pollution, and toxic mine drainage place water resources under continuous pressure and
32 pose a serious threat to the biodiversity of the wetland. Within this context of water scarcity, climate
33 change is likely to exacerbate water resource shortages. Consequently, groundwater will become
34 increasingly important in conserving riparian ecosystems and groundwater dependent wetlands.
35 These issues have made the scientific community (Custodio et al. 2007), management authorities
36 (Junta de Andalucía 2009), and environmental organizations (WWF España 2006) consider how
37 policies for the management of the Doñana wetland and its surrounding areas, which have been
38 designated as both a National Park and a UNESCO World Heritage Site, can include climate change
39 mitigation and adaptation measures.

40 In relation to water resources it is expected that climate change will result in increasing
41 evaporation, more intense periods of precipitation, and more extreme hydrological events such as
42 floods and droughts (IPCC 2007). Global climate models (GCMs) project mean annual increases in
43 temperature of between 1.2 and 7.4°C in the Doñana area for the 2071–2100 time-slice (IPCC
44 2007). Projections of changes in precipitation are less well constrained and the GCM outputs
45 indicate that there is uncertainty about the sign of the change.

46 Over the last decade, an extensive amount of research has been published on how climate
47 change might affect different aspects of the hydrological cycle, as reviewed by Bates et al. (2008),
48 and impacts on groundwater resources are receiving greater attention (Dragoni and Sukhija 2008).
49 Most of the research examining groundwater-related climate effects has used physically-based or
50 empirical models to simulate groundwater system response to a change in climate. Whichever
51 approach is adopted, it is necessary to quantify the change in precipitation and temperature under
52 future conditions. This can be done by constructing plausible scenarios that are informed by the

53 range of regional climate model (RCM) and GCM outputs (e.g., Woldeamlak et al. 2007) or by
54 downscaling individual GCM outputs to the catchment scale (e.g., Segui et al. 2010). Few studies of
55 the effects of climate change on groundwater have used ensembles of more than three different
56 scenarios in their assessment (Eckhardt and Ulbrich 2003; Woldeamlak et al. 2007; Goderniaux et
57 al. 2009; Jackson et al. 2011).

58 Relatively few studies have examined the effects of climate change on groundwater resources
59 in Spain. Manzano et al. (1998) estimated decreases in recharge of up to 16% for Mallorca for the
60 period 1992–2040 compared to 1974–1988. Younger et al. (2002) simulated decreases in mean
61 recharge of up to 8% and 16% for aquifers in Cataluña and Mallorca, respectively, by 2036–2045
62 relative to pre-1995 values. Custodio et al. (2007) performed a preliminary analysis to quantify the
63 effects of climate change on the Doñana area from empirical formulas of evapotranspiration. More
64 recently, Aguilera and Murillo (2009) examined twentieth century recharge rates and identified
65 decreasing trends in decadal mean recharge for four karstic aquifers in Alicante. Candela et al.
66 (2009) applied two different climatic scenarios developed by the Intergovernmental Panel on
67 Climate Change (IPCC 2000) to examine the effects of climate change and management scenarios
68 on the Inca-Sa Pobla coastal aquifer, Mallorca and its associated wetland. GCM outputs were used
69 to quantify recharge and drive a numerical model of the aquifer, for which overall decreases in
70 natural recharge ranging from 4% to 21% by 2025 were simulated. In Doñana, Guardiola-Albert et
71 al. (2009) investigated how groundwater outputs vary depending on the occurrence of dry, medium,
72 or wet years.

73 Considering climate change pressures, and the importance of managing water resources
74 effectively for ecosystem services within the Doñana area, this paper addresses the issue of GCM
75 uncertainty in an evaluation of the impact of climate change on groundwater resources. First, we
76 examine the potential impacts on groundwater recharge in the Almonte-Marismas aquifer. Second,
77 we analyse the impact of a change in climate of southern Spain on the hydrogeological system, in
78 particular on the groundwater discharge into the streams flowing into the marshland. The study used

79 outputs from 13 GCMs (Table 1) available from the IPCC Data Distribution Centre for the 2080s
80 under the A2 emission scenario (IPCC 2000) to generate future downscaled sequences of
81 precipitation and potential evaporation (PE) by perturbing historic sequences of these variables.
82 This provides an indication of the level of confidence to be attached to the results of the impact
83 assessment. These projected climatic variables were used to drive distributed recharge and
84 groundwater flow models and calculate changes in rainfall recharge, groundwater levels in the
85 aquifer and in groundwater discharge into the streams flowing into the marshland.

86 **2. Study area**

87 **2.1. Location and physiography**

88 The Doñana wetland, located in the south-west Iberian Peninsula (Figure 1a), is considered one of
89 the most important in Spain (Serrano et al. 2006). It extends along the coast between the estuaries of
90 the Guadalquivir and Tinto rivers, and inland to the uplands of “El Aljarafe” (Sevilla). It covers an
91 area of approximately 1000 km² within which there are regions with different levels of
92 environmental protection. Apart from the marshland the area has a large number of small,
93 temporary lagoons (Sousa and García Murillo 1999).

94 At the same time, the Doñana region constitutes an area containing a wide variety of
95 competing water resource demands necessary to maintain agriculture, industry, mining, and
96 tourism. Since the late 19th century different kinds of human activity have significantly changed the
97 natural environment. The area of marshland has decreased from 1400 km² to the 270 km² that
98 remain in a semi-virgin state today (Rodríguez-Rodríguez et al. 2006).

99 The topography of the region falls from approximately 150 m above sea level (m aSL) in the
100 north to less than 1 m aSL in the marshland area near the coast in the south. To the south fossil sand
101 dunes form coastal cliffs over 100 m high that are retreating due to coastal erosion. Rivers and
102 streams flow from the higher regions in the north towards the marshland as does the Guadiamar
103 River, which drains a complex of extensive tributaries including the El Gato and Alcarayón streams.
104 In the north-west of the region the La Rocina, El Partido, and La Cañada water courses drain

105 southwards into the marshland.

106 The Doñana area comprises three large ecosystems: stabilised sands or cotos, a sand dune spit
107 running parallel to the coast-line, and the marshland. The contact between the dune sand and
108 marshland areas constitutes a seepage limit in La Vera-Retuerta (Serrano et al. 2006), an
109 ecologically important area which provides moisture to grass meadows and hydrophitic vegetation,
110 and feeds small creeks especially during periods of heavy rainfall. Much of the study area is
111 covered by pine, although at the beginning of the 20th century a large number of economically
112 valuable eucalyptus trees were planted. These had a significant impact on groundwater levels
113 because of their high water demand. From the mid-1990s eucalyptus started to be cut down, but
114 approximately 6400 ha remain today.

115 **2.2. Hydrogeology**

116 The Almonte-Marismas aquifer system (Figure 1b) covers 2640 km² of the south western part of the
117 lower Guadalquivir basin. It is composed of Miocene and Quaternary sediments: silt, sand, and
118 gravel (Trick and Custodio 2004). The alluvial deposits of fine materials located in El Abalarío are
119 partially covered by aeolian sands, while in the central plain they are covered by estuary and
120 marshland silt and clay containing some sand and gravel, with a total thickness of up to 100 m
121 (Figure 1c). The depth of the aeolian sands varies from over 100 m at the coast to approximately
122 10 m at the northern edge of the region. Groundwater predominantly circulates from the north-east
123 to the south and then east before discharging to the Atlantic Ocean or north into the La Rocina
124 stream, the main permanent tributary to the marshland. The aquifer system of Almonte-Marismas
125 drains into the Tinto River, along the coast, and into temporary pools and springs that drain into the
126 marshland. Groundwater abstraction for irrigation amounts to 60–90 hm³ year⁻¹ (1 hm³ = 10⁶ m³),
127 causing decreases in the piezometric level and reductions in groundwater contributions to the
128 streams supplying the marsh during the summer. Agriculture is concentrated in three areas: around
129 El Rocío village, between the coast and the Tinto River, and across the north-east boundary of the
130 marshes. In the first two of these areas strawberries and citrus fruits are the main crops, and

131 groundwater is the principal source of water for irrigation. In the third area rice and cotton are the
132 main crops, which are irrigated with both river water and intensively abstracted groundwater.
133 Groundwater is also abstracted to supply the towns and the tourist resorts of Mazagón and
134 Matalascañas ($3\text{--}6 \text{ hm}^3\text{year}^{-1}$), with an associated impact on the wetland.

135 The permeability of the main geomorphological units is very different: the aeolian sands
136 correspond to an unconfined aquifer (with a shallow water table and several flow systems) while
137 groundwater is confined below the silty-clay deposits of the floodplain. The relatively thick aeolian
138 sand deposits, which are occasionally inter-layered with finer sediments, form a relatively low
139 permeability, unconfined upper aquifer with a shallow water table. This overlies a thinner, and more
140 heterogeneous, lower aquifer that becomes leaky-confined beneath the marshland silt and clay
141 (Trick and Custodio 2004). The transmissivity of the lower aquifer is higher than that of the upper
142 aquifer, due to the presence of layers containing coarse sand and gravel. The aquifer system is
143 underlain by impermeable marine marls. The transmissivity of the aquifer increases from north to
144 south, varying from on average $100 \text{ m}^2\text{d}^{-1}$ around Almonte to $3000 \text{ m}^2\text{d}^{-1}$ beneath the marshland
145 (FAO 1975; Trick and Custodio 2004). In the unconfined aquifer effective porosity varies between
146 2 and 5 %. Confined storage coefficient values are in the range 10^{-3} to 10^{-4} (IGME 2009).

147 Most of the recharge is derived from rainfall over the unconfined aquifer, irrigation return
148 flow, and by lateral inflow from the Aljarafe aquifer. Recharge, which is produced during spring
149 and autumn predominantly, has been estimated to total $200 \text{ hm}^3\text{year}^{-1}$ (IGME 1992) on average. The
150 confined aquifer beneath the marshland is fed by lateral groundwater flow. Groundwater discharges
151 from the aquifer through the rivers and streams, via lateral flow to the sea, evapotranspiration,
152 leakage at the dune-marshland margin, and to a lesser extent via upflow through the silt and clay to
153 the marshland. Groundwater abstraction for agricultural and industrial use and for public supply is
154 also significant and has reversed the direction of groundwater flow in some areas, such as in the
155 north-eastern part of the marshland (UPC 1999).

156 **3. Methods**

157 The methodology applied to quantify the potential effects of climate change on the Doñana wetland
158 system is summarised in four stages:

- 159 1. Future time-series of catchment precipitation and temperature were calculated by perturbing
160 historic time-series of these variables using monthly *change factors*. These change factors
161 represent the difference between a GCM simulation of the reference climate, 1961–1990, and a
162 future climate, which in this study is the period 2071–2100 under the A2 emissions scenario
163 (IPCC 2000). Here we applied monthly change factors derived from 13 GCMs reported in the
164 IPCC Fourth Assessment Report (IPCC 2007).
- 165 2. The 13 time-series of future precipitation and potential evaporation (calculated from the
166 temperature) were used to drive a ZOODRM (Mansour and Hughes 2004) distributed
167 groundwater recharge model of the area.
- 168 3. Each future recharge time-series was used as input for a calibrated MODFLOW (McDonald
169 and Harbaugh 1988) groundwater flow model of the Almonte-Marismas aquifer. All of the
170 other groundwater model parameters remained the same as the baseline run from 1975 to 1997.
- 171 4. Changes in state variables between the baseline and 13 future simulations were calculated.

172 **3.1. Climate change scenario generation and downscaling**

173 In this work the A2 greenhouse gas emissions scenario (IPCC 2000) was applied. This medium-
174 high emissions scenario is based on a socio-economic storyline that supposes a world of
175 independently operating, self reliant nations with continuously increasing global population and
176 regionally oriented economic growth that is more fragmented and slower than in other storylines
177 (IPCC 2000). The simulated climate based on this scenario was derived from the 13 GCMs listed in
178 Table 1, which are reported in the Fourth Assessment Report of the IPCC (IPCC 2007).

179 GCMs do not accurately simulate local climate, but the internal consistency of these
180 physically-based climate models means that they provide the current best estimate of the ratios and
181 differences (scaling factors) of future precipitation and temperature from historical (base case)
182 records. A number of different spatial and temporal downscaling techniques can be used to derive

183 finer resolution climate information from coarser resolution GCM output, for example based on
184 statistical methods (e.g., Wilby et al. 1998) such as stochastic weather generators (Kilsby et al.
185 2007), or dynamical downscaling using regional climate models (Graham et al. 2007). The simplest
186 method for modifying time series of catchment model driving data using GCM outputs is the delta
187 change or change factor (CF) method (Wilby and Harris 2006). For a given variable, the difference
188 between the simulation by a GCM of a reference climate and a future climate are used to adjust
189 sequences of catchment model driving variables. Whilst the CF approach offers a robust method to
190 compare average outcomes from different climate models, it cannot provide any information on
191 changes in hydrological extremes (Graham et al. 2007) because it assumes that the variability of the
192 climate remains unchanged in the future. However, the CF method remains one of the most widely
193 used for analysis of climate change impact on non-extreme variables and was used here to quantify
194 changes in the monthly means of state variables. Change factors were used to perturb historic
195 sequences of daily rainfall and monthly PE. The 2080s time horizon was selected because it has the
196 strongest ratio between the signal of change and natural variability and the A2 emissions scenario
197 (IPCC 2000) was applied because it is one of the most commonly considered scenarios. Simulated
198 changes in mean monthly temperature and rainfall between the 1961–1990 and 2071–2100 periods
199 for the A2 scenario were used. These factors were obtained for the 13 GCMs from the IPCC Data
200 Distribution Center (http://www.ipcc-data.org/ar4/gcm_data.html). Because the middle of the
201 baseline period for the catchment simulation (1975–1997) differs from that of the climate model
202 baseline (1961–1990) by 10.5 years, the monthly change factors were adjusted to account for this.
203 This has been done by linearly scaling the factors assuming that the rate of change of temperature
204 and precipitation is constant over time. The resulting perturbed time-series of driving climate
205 variables were applied to the ZOODRM distributed recharge model, which calculated recharge for
206 the transient groundwater flow model of the Almonte-Marismas aquifer.

207 **3.2. Recharge estimation**

208 Groundwater recharge was calculated using the gridded ZOODRM model (Mansour and Hughes

209 2004). ZOODRM has been applied to a wide variety of hydrological regimes within temperate and
210 semi-arid regions (Hughes et al. 2008; Jackson et al. 2011). The model uses a soil moisture balance
211 approach based on the FAO method (FAO 1998) to calculate, evapotranspiration, surface runoff,
212 and recharge using spatially distributed daily rainfall and potential evaporation time-series and land
213 surface elevation, land-use, and geological data. A digital terrain model is used to route runoff
214 across the land surface, which can subsequently infiltrate to form indirect recharge. The proportion
215 of rainfall forming runoff is related to the topography, soil type, and geology.

216 Lerner et al. (1990) provided a method for determining if soil moisture budgeting methods are
217 applicable to a given terrain. This requires that potential evaporation is less than 1.5 and 3 times the
218 amount of precipitation plus irrigation during the wet and dry seasons, respectively. This criterion is
219 not met during the dry season within the Doñana area but because very little recharge occurs during
220 the summer months, due to the large disparity between PE and precipitation, the approach remains
221 acceptable. Calculated recharge rates have been found to be comparable to those derived by
222 Guardiola-Albert et al. (2005) who calculated mean recharge to be 0.2 mm d^{-1} using soil water
223 balance methods and inverse groundwater modelling (UPC 1999).

224 The baseline period was simulated using a network of 22 rain gauges with daily time series.
225 Rainfall was distributed in space by comparing the long-term average rainfall at a grid node with
226 that at an associated rainfall station. Grid nodes were associated with a rainfall station by
227 constructing Thiessen polygons around the rainfall gauges. The distribution of long-term average
228 rainfall in space was constructed by kriging the point long-term average values at the rain gauges to
229 produce a surface.

230 The temperature time-series for the 19 meteorological stations within the model area are very
231 similar and therefore, a single temperature time-series was used to construct a record of potential
232 evaporation. The Palacio de Doñana (Figure 1a) temperature record, which covers the period
233 November 1978 to March 2007, was used to calculate PE. The Los Palacios y Villafranca station
234 has a reference evaporation (ET_0) record, based on measured meteorological variables, from

235 October 2000 to July 2007. Using Palacio de Doñana temperature data over the same period, a PE
236 time-series was constructed using the Blaney Criddle method (Allen and Pruitt 1986). Monthly
237 Blaney Criddle k values were calibrated by fitting the calculated PE time-series to the measured
238 ET_0 values. The comparison between the monthly mean measured ET_0 values and the calculated PE
239 values is shown in Table 2. The daily consumptive use coefficient, k, which depends on the
240 vegetation type and season, was interpolated from the monthly values to avoid the occurrence of
241 step changes in PE between months. A time-series of PE was subsequently constructed for the full
242 baseline period between January 1975 and December 1997 using the full Palacio Doñana
243 temperature record. It was assumed that the period January 1975 to October 1978, for which there
244 are no temperature data, is equivalent to the period from January 1983 to October 1986, which is
245 characteristic of a non-extreme period of temperature variations.

246 The spatial distribution of vegetation was assumed to be constant during the baseline and
247 future modelling periods and based on 15 zones derived from land-use data for 1999. In eight of
248 these zones the FAO method for calculating recharge was applied and crop parameter values were
249 based on those specified in the FAO guidelines (FAO 1998). Within the remaining seven zones
250 there were insufficient data to implement the FAO method and therefore the Penman-Grindley
251 (Penman 1948; Grindley 1967) soil moisture deficit method (SMD) was applied. The Root
252 Constant, C, and Wilting Point, D, parameters used in the SMD method were based on values
253 presented by Lerner et al. (1990) but were adjusted during the model calibration process. Run-off is
254 routed across the land surface according to topographic elevation. The percentage of rainfall
255 becoming run-off varies across the model, and was defined using zones. These zones were based on
256 the hydraulic conductivity classification of the surface geology.

257 The ZOODRM model was calibrated by comparison against detailed groundwater balances
258 obtained in previous studies (Guardiola-Albert et al. 2005). The spatially-distributed and
259 temporally-varying recharge series calculated by the ZOODRM model for the baseline period and
260 the 13 future climates formed input to the groundwater flow model of the Almonte-Marismas

261 aquifer.

262 **3.3. Almonte-Marismas groundwater flow model**

263 The numerical groundwater flow model was constructed using the MODFLOW code (McDonald
264 and Harbaugh 1988). The model grid covers an area of 2600 km² and was divided into two layers
265 and a uniform horizontal mesh of 500 m square cells. The upper layer represents the thick sand
266 deposits, occasionally inter-layered with finer sediments and the lower layer represents the
267 heterogeneous sand and gravel lower aquifer. The base of this two-layer aquifer system coincides
268 with the top of the underlying low permeability Miocene marls.

269 The limits of the model were defined along physically justifiable boundaries. In the south the
270 Atlantic Ocean was represented by a series of constant head cells. In the north a constant flow
271 boundary condition was specified along the edge of the outcrop of the marls, which coincides with a
272 line of springs. In the north-east a constant flow boundary condition was specified representing
273 groundwater flow from the Aljarafe aquifer, the rate of which was based on estimates of
274 transmissivity from pumping test data and groundwater head gradients from levels in observation
275 boreholes. Elsewhere the groundwater model boundaries were defined as no-flow, however, a
276 number of head-dependent boundary conditions were also set within the model (Figure 2). In the
277 east groundwater discharges to the Guadalquivir River through a series of MODFLOW *river cells*.
278 River cells were also included in the model to simulate flows to the Tinto River in the north-west
279 and the Gudiamar River in the north-east. *Drain cells* were used to model the marshland area and
280 discharges to the associated ecotone (seepage limit), along the border with the dune sand aquifer,
281 and to coastal springs in the south. The network of intermittently flowing watercourses within the
282 study area was modelled using MODFLOW *stream cells* (Prudic et al. 2004). Groundwater
283 abstractions for irrigation and water supply were included in the model, the location and pumping
284 rates of which were based on monitored data. This totals on average approximately 47 hm³year⁻¹.

285 The hydraulic parameters of hydrogeological zones within the model, based on the geology
286 (Figure 1b), were specified initially using data from more than 400 pumping tests but adjusted

287 during the calibration of the model against observed groundwater heads (Guardiola-Albert et al.
288 2005). Model hydraulic conductivity values range from 0.001 to 50 m day⁻¹. Initially a steady-state
289 model was calibrated to historic mean groundwater levels in over 300 boreholes. Subsequently a
290 time-variant model of the period 1975-1997 was developed. Simulated groundwater level time-
291 series were compared to data from more than 1000 observation boreholes in the study area. The
292 comparison between the simulated and observed groundwater levels at four of these boreholes is
293 shown in Figure 3. A decrease in groundwater levels caused by the introduction of intensive
294 irrigation is clearly identifiable within the marshland area (borehole 4).

295 The following error measures were used to evaluate the goodness of fit of the calibration of
296 the model: mean error (ME), mean absolute error (MAE), and standard root mean square error
297 (SRMSE). Anderson and Woessner (1992) consider that an acceptable fit to the observed data is
298 achieved when the ME and SRMSE values are less than 0.5 m and 10%, respectively. These head
299 error measures for the numerical model of the Almonte-Marismas aquifer are listed in Table 3.
300 These values indicated that the calibration was more than acceptable. Another indicative parameter
301 of the acceptability of the simulation was the mass balance error, which was considered to be
302 admissible when its value is around 1% of the total inflow (De Marsily 1986). The maximum values
303 of the absolute differences between the inputs and outputs obtained in the steady-state and transient
304 simulations were 0.02 and 0.15%, respectively.

305 **3.4. Groundwater simulations with GCM projected climate**

306 Each of the future recharge series, calculated by the ZOODRM code using the climate output from
307 the 13 GCMs, were input into the groundwater flow model. All other model stimuli and parameters
308 remained the same as the baseline (1975-1997) run. Consequently, it was assumed that changes in
309 groundwater abstraction and management practice do not change between the baseline period and
310 the 2080s. The transient groundwater model simulates fluctuations in groundwater level, and
311 groundwater discharge to the rivers, marshland, and sea. The comparison between the baseline
312 simulation and the future simulations was made by calculating differences in recharge, groundwater

313 levels, and the components of the flow balance.

314 **4. Results**

315 **4.1. Projected climatology and impacts on groundwater recharge**

316 *Temperature and potential evaporation*

317 Figure 4 shows the projected increase in mean monthly temperature from the baseline period
318 (Table 2) for each of the 13 GCMs. All of the GCMs project a warming of at least 1.2°C for each
319 month for the Doñana area. Between the months of November and March the increase, described by
320 the average of the ensemble of models (black line in Figure 4), varies between 2.4 and 3.5°C.
321 Between the months of April and October this ensemble average increase ranges from 4.2 to 4.7°C.
322 Projected temperature increases are much higher during the summer, reaching a maximum value of
323 7.4°C for the HADCM3 model projection. The CSMK3 model projects the smallest increase in
324 temperature of between 1.0°C in February and 2.3°C in September.

325 The calculated increases in monthly average PE for the 2080s from the baseline period are
326 shown Figure 4. Percentage increases in PE are highest between the months of May to October with
327 ensemble average values of between 11.2 and 13%. The CSMK3 model projects the smallest
328 monthly increases in PE for the Doñana area of between 4.0 and 6.5%. The HADCM3 model
329 projects the greatest monthly increases of PE between 10.0 and 20.8%.

330 *Precipitation*

331 Figure 4 shows the projected changes in mean monthly precipitation for the 2080s from the baseline
332 period (Table 2) for each of the GCMs. Negative values represent a decrease in precipitation and
333 vice versa. The monthly averages of the ensemble change factors suggest a decrease in precipitation
334 throughout the whole year with a maximum decrease of 0.51 mm d⁻¹ in November. Uncertainty in
335 the projection of the change in rainfall is greatest in winter with some GCMs projecting an increase
336 in rainfall and some a decrease. As would be expected, reductions are generally projected to be less
337 in summer when rainfall rates are low.

338 A number of GCMs project significant changes in precipitation during the winter. For

339 example, the IPCM4 model projects an increase of 0.4 mm d^{-1} in the months of February and
340 March, HADCM3 an increase of 0.4 mm d^{-1} in December, and CNCM3 an increase of 0.35 mm d^{-1}
341 in September. A decrease of 1.3 mm d^{-1} is projected by the GFCM20 model in February and April
342 and CNCM3 projects a decrease of 1.2 mm d^{-1} in November. All models project changes between -
343 0.11 and $+0.09 \text{ mm d}^{-1}$ in August.

344 ***Recharge***

345 Figure 5 shows the monthly mean values of recharge for all the 13 future simulations and the entire
346 modelled area, as well as the average of the ensemble and the historic mean, simulated using
347 ZOODRM. Mean monthly recharge during the baseline period varies from 0.93 mm d^{-1} in February
348 to none in July and August. Decreases in mean monthly recharge are produced for at least nine
349 months of the year in all 13 future simulations. Six of the 13 future simulations produce reductions
350 in mean monthly recharge over the whole year. The most pronounced decrease, of 0.57 mm , is
351 simulated in December using the GFCM20 climate projection. For all models the largest reduction
352 in recharge, as a percentage, occurs in April. Bootstrapped 95% confidence intervals on the
353 ensemble mean of the percentage changes in mean November recharge are -44 and -23% . For mean
354 December recharge, these confidence intervals are -44 and -24% .

355 Annual recharge, expressed by the average of the ensemble of the 13 future simulations, is
356 simulated to decrease by 35%. However the spread of the simulations ranges from a 57% decrease
357 using the CNCM3 projection to a 14% decrease using the HADCM3 and NCPCM projections.
358 Bootstrapped 95% confidence intervals on the ensemble mean of the percentage changes in mean
359 annual recharge are -43 and -27% . These values are similar to that estimated by Custodio et al.
360 (2007) in Doñana area, that suggest a decrease of recharge of 50% for an increase of temperature of
361 1°C .

362 **4.2. Climate change impacts on groundwater levels**

363 Figure 6 depicts differences in groundwater levels across the aquifer for December 2084 relative to
364 the December 1979 in the baseline period. This date was selected as the monthly rainfall is close to

365 the average rainfall in the area and also because it follows a period which was not very dry or wet.
366 The differences in groundwater level across the aquifer range between -17 and +2 m at this time.

367 Absolute differences in groundwater level between the baseline and future simulations across
368 the northern part of the Almonte-Marismas aquifer and over some areas of the marshland are less
369 0.5 m (see white areas in Figure 6). The largest reductions in groundwater level, of up to 17 m, are
370 simulated across the unconfined groundwater mound in the El Abalario region. Other areas where
371 there are significant simulated declines in the water table include the upper catchment of La Rocina
372 stream (-1 to -5 m) and the irrigated Los Hatos region (-1 to -3 m). There is not a zone in which
373 there is a significant rise of water levels in any of the simulations. The GFCM21 simulation
374 produces the greatest decreases in water levels in comparison with the baseline simulation, with
375 declines of up to 17 m. The NCPCM simulation is most similar to the baseline with decreases of up
376 to 5 m in El Abalario. In general, for the 13 future simulations, water levels under the marshland
377 tend to decrease between 0 and 6 m, but this fact has to be considered along with the reduction in
378 discharge from the aquifer to the streams that flow into the marshland. In the irrigated Los Hatos
379 area the maximum decline in groundwater level is 4 m under the GFCM21 simulation.

380 The simulations show that there is an impact on changes to hydraulic head in terms of the
381 overall water table configuration. Changes in groundwater level increase significantly away from
382 the coast to the north (Figure 6). Some areas of the marshland are less affected by the change in
383 climate. However, there are notable differences in the groundwater table configuration between the
384 future simulations and the baseline, accounting for the redistribution of water within the system.

385 **4.3. Preservation of groundwater ecological discharges**

386 ***Groundwater discharge to streams feeding the marshland***

387 For each future simulation temporal changes in the water balance have been calculated to examine
388 the exchange of water between the aquifer and the main streams and drains that maintain the
389 marshland: Guadiamar, Marismas, El Partido and La Rocina (Table 4). Whilst on average, flows
390 from the streams to the aquifer do not change significantly with respect baseline values,

391 groundwater contributions to stream flows in the Marismas and La Rocina basins are considerably
392 diminished by on average 53% and 36%, respectively. The discharge from the aquifer to the
393 Guadiamar and El Partido basins, again as represented by the ensemble average, decreases by 7%
394 and 15%, respectively, compared to the baseline values. Similar behaviour was also described in the
395 preliminary study of Guardiola-Albert et al. (2009) in which climate change impacts were shown to
396 have a more significant effect on groundwater outflows to rivers than river flows returns to the
397 aquifer. This can be explained by the fact that during dry periods the streams are disconnected from
398 the aquifer. During dry periods groundwater recharge and storage are reduced resulting in water
399 table declines. As a result baseflow is reduced, and when the water table lies below the streambed
400 there is a disconnection between the stream and the aquifer.

401 All the 13 models simulate lower values than the historic rates throughout the year and a
402 dampening of the seasonal pattern of flows to the marshland. The most severe reduction in flow to
403 the marshland of 26.7 hm³/y is simulated using the outputs from CSMK3. These large reductions in
404 groundwater discharge to the marshland, combined with the predicted decreases in baseflow in the
405 La Rocina stream baseflow, represent a major decrease of water supply to the Doñana ecosystem.
406 Similar impacts have been reported for other southern Spanish wetlands (Rodríguez-Rodríguez et
407 al. 2006).

408 ***Groundwater discharge to the sea***

409 To evaluate the outputs to the sea, simulated flows flow from the springs associated with cliffs on
410 the coast and flows to the constant head boundary are combined. The resulting changes in monthly
411 average discharges to the sea are shown in Figure 7. The simulations indicate a decrease of coastal
412 groundwater discharge throughout the whole year, with an ensemble mean decrease of 35%. Some
413 future simulations however (e.g., GFCM21) suggest decreases of more than 50%. Although not
414 assessed here, such changes would result in enhanced saline intrusion and deteriorations in
415 groundwater quality.

416 **5. Discussion**

417 In general, the results of this modelling study indicate that the change in climate by the 2080s, will
418 lead to a reduction in groundwater resources. Mean annual recharge rates are simulated to decrease
419 by between 14 and 57% using the different GCM projections. The average of the ensemble of future
420 simulations suggests that monthly recharge will decrease throughout the year. These decreases in
421 recharge result in significant reductions in groundwater heads and changes in the water table
422 configuration. Decreases in groundwater level depend on the simulation and the location but can be
423 as much as 17 m over the unconfined interfluvial regions. Whilst the future simulations suggest a
424 change in the seasonal distribution of recharge to the aquifer, this does not translate into a
425 significant change in the distribution of mean monthly groundwater levels. This seems to indicate
426 that climate change will lead to a monotonic decrease of groundwater levels rather than a significant
427 impact on seasonal fluctuations of groundwater levels. However, this result must be considered in
428 the context of the use of the change factor approach in this study which only perturbs the monthly
429 means of the driving climate variables and not the variability of the future climate.

430 Such declines in groundwater level result in a reduction of groundwater flow into the streams
431 and to the marshland and an obvious reduction in the availability of water required to maintain
432 aquatic life in the wetland and riparian ecosystems, especially in summer (Trick and Custodio 2004;
433 Custodio et al. 2007). All 13 future simulations indicate decreases in discharge, of up to 68%, from
434 the aquifer to the La Rocina and Marismas basins, which form the main water supplies to the
435 marshland during the summer and which sustain important ecological systems. The consequences
436 of these baseflow reductions, together with the decrease of direct discharge from aquifer to
437 marshlands, could be drastic as it would reduce the availability of water that is necessary for the
438 maintenance of aquatic life in the wetland and riparian ecosystems, especially during summer
439 (Serrano et al. 2006). In addition, for the La Rocina stream, the amount of water flow has
440 approximately halved within the last 20 years as a consequence of strawberry farm encroachment
441 and the associated interception of groundwater. Hence, as discussed by Primack (2000) and WWF
442 España (2006) climate change is another factor limiting the width of the riparian corridor along the

443 stream, and its effect must be considered within management plans developed by the water resource
444 regulators and stakeholders. As suggested by Custodio et al. (1994), predicted decreases in
445 discharge rates from the aquifer to the sea, of more than 50% by some models, would also result in
446 the advance of saline water inland.

447 To put the potential effects of climate change on the Doñana wetland into context, a
448 comparison has been made between the simulated impacts and current groundwater abstraction
449 rates within the region. Simulated minimum, ensemble average and maximum decreases in total
450 groundwater discharge (MODFLOW stream cell plus drain cell leakage) to the La Rocina, El
451 Partido and Las Marismas basins are presented (Table 4). Groundwater abstraction in each of these
452 catchments, for both irrigation and public supply, is also given. Mean historic total groundwater
453 abstraction rates in the La Rocina, El Partido, Las Marismas and Guadiamar basins are 8.0, 0.3,
454 18.6, and 0.1 hm³/year, respectively. These are equivalent to 24, 3, 47, and 1% of the historic
455 groundwater discharge to each catchment, respectively. Decreases in groundwater discharge to the
456 basins due to climate change are significantly greater than historic rates of abstraction in both the La
457 Rocina and Las Marismas basins. In the El Partido basin one of the future simulations produces a
458 4% increase in mean groundwater discharge but the worst case simulation produces a 73%
459 reduction in groundwater discharge. The ensemble averages of the 13 future simulations represent
460 decreases in groundwater discharge to these four basins of between 7 and 53% of mean historic
461 discharge rates. These values provide the following useful guidelines to water and wetland policy-
462 makers and stakeholders: (i) simulated climate induced decreases in groundwater discharge to the
463 surface are substantive in comparison to the current wetland groundwater balance, (ii) these
464 decreases are proportionally greater in the La Rocina and Las Marismas basin, than in the El Partido
465 and Guadiamar basins, (iii) modelled reductions in groundwater flow to the surface associated with
466 climate change are greater than current groundwater abstraction rates in most of the future
467 simulations, and (iv) in the larger La Rocina and Las Marismas catchments, however, simulated

468 worst case decreases in groundwater discharge to the surface are 2.4 and 1.5 times greater than
469 current abstraction rates, respectively.

470 This work has neglected possible changes in land-use, groundwater abstraction, and water
471 resource management that may occur in response to a need to adapt to the changing climate and the
472 results must be considered in the context. It is necessary to underline that all investigations for this
473 study were realised on a regional scale and thus conclusions drawn also have to be regarded in this
474 context. Nevertheless, it seems realistic to claim that climate change is likely to have a dramatic
475 impact on groundwater resources, due to the combined effect of direct and indirect factors. Despite
476 all efforts to mitigate climate change, there will be a need to implement significant adaptation
477 measures to minimise the effect of climate change on groundwater resources (WWF España 2006).

478 The analyses presented here focus on the direct impact of climate change on groundwater
479 resources, which have been simulated to be potentially large. The results have shown that GCM
480 uncertainty is significant in the assessment of the potential impacts of climate change on this
481 internationally important wetland. However, the direction of the change is consistent across all 13
482 of the future simulations. The spread of the change in mean recharge for the 2080s time-slice is
483 bounded by simulated decreases of 14 and 57%. Furthermore, bootstrapped 95% confidence
484 intervals on the average of this ensemble of simulated changes in mean recharge are -43 and -27%.
485 Therefore, the results suggest that a significant change in the hydrological regime will occur over
486 the coming century. Importantly, this result has been placed within the context of the current
487 exploitation of the groundwater resource. Decreases in groundwater discharge to the surface water
488 basins supplying the marshland have been simulated to be greater than current groundwater
489 abstraction rates in the large majority of the future simulations. Consequently, even if the use of
490 groundwater for public supply and irrigation is stopped, the supply of groundwater to the wetland is
491 likely to diminish. Further studies are required to put the impact of climate change on groundwater
492 resources within the context of human exploitation of groundwater resources.

493 Whilst these findings neglect other human induced effects such as changes in water use,

494 groundwater abstraction, and land-use and soil degradation, the methodology provides a practical
495 and useful way to generate a physically based evaluation of the impacts of climate change on a
496 groundwater system. As suggested by Kuhn et al. (2011) to provide a more complete understanding
497 of the impact of climate change on wetland systems it will be necessary to consider indirect effects,
498 such as changes in land use, irrigation, and groundwater exploitation. To improve the assessment of
499 the impacts on this wetland of great ecological importance there is an urgent need to develop a
500 complete water balance model based on a fully coupled surface water-groundwater model.

501 **6. Acknowledgments**

502 This study was undertaken as part of the “Improvement of the Almonte-Marismas mathematical
503 model as a supporting tool for water resources management” project funded by the Spanish
504 Geological Survey. Some additional funding was provided through the NERC-BGS core science
505 budget. The authors would like to thank C Prudhomme at the Centre for Ecology and Hydrology,
506 UK, for assistance in processing GCM output. C.R. Jackson publishes with the permission of the
507 Executive Director of the British Geological Survey.

508 **7. References**

- 509 Aguilera H, Murillo JM (2009) The effect of possible climate change on natural groundwater
510 recharge based on a simple model: a study of four karstic aquifers in SE Spain. *Environmental*
511 *Geology* 57:963–974
- 512 Allen RA, Pruitt WO (1986) Rational Use of the FAO Blaney-Criddle formula. *Journal of Irrigation*
513 *and Drainage Engineering, ASCE* 112: 139–155
- 514 Anderson MP and Woessner WW (1992) *Applied groundwater modelling*. Academic Press, San
515 Diego
- 516 Bates B, Kundzewicz ZW, Wu S, Palutikof JP (2008) *Climate change and water*. Technical paper of
517 the Intergovernmental Panel on Climate Change, IPCC Secretariat. Geneva
- 518 Candela L, von Igel W, Elorza FJ, Aronica G (2009) Impact assessment of combined climate and
519 management scenarios on groundwater resources and associated wetland (Majorca, Spain).

520 *Journal of Hydrology* 376: 510–527

521 Custodio E, Iglesias M, Manzano M, Trick T (1994) Saltwater intrusion risk along the western
522 Donana area cost (Southwestern Spain). 13th Salt Water Intrusion Meeting. Universita deli Studi
523 di Cagliari, Italy: 286–303

524 Custodio E, Manzano M, Escaler I (2007) Aquifer recharge and global change: application to
525 Doñana. *El cambio climático en Andalucía: evolución y consecuencias medioambientales*. Junta
526 de Andalucía Publication: 121–140

527 Custodio E, Manzano M, Montes C (2009) Las aguas subterráneas en Doñana: aspectos ecológicos
528 y sociales. Agencia Andaluza del Agua, Spain

529 De Marsily G (1986) *Quantitative Hydrogeology*. Academic Press, San Diego

530 Dragoni W, Sukhija BS (2008) Climate change and groundwater: a short review. Special
531 Publication No. 288. The Geological Society, London, pp 1–12

532 Eckhardt K, Ulbrich U (2003) Potential impacts of climate change on groundwater recharge and
533 streamflow in a central European low mountain range. *Journal of Hydrology* 284:244–252

534 FAO (1975) Proyecto piloto de utilización de lagunas subterráneas para el desarrollo agrícola de la
535 cuenca del Guadalquivir. Proyecto de transformación de la zona regable Almonte-
536 Marismas. Technical Report. AGL:SF/SPA 16. Rome

537 FAO (1998) Crop evapotranspiration; Guidelines for computing crop water requirements. Food and
538 Agriculture Organization of the United Nations Irrigation and Drainage Paper 56, Rome

539 Goderniaux P, Brouyere S, Fowler HJ, Blenkinsop S, Therrien R, Orban P, Dassargues A (2009)
540 Large scale surface-subsurface hydrological model to assess climate change impacts on
541 groundwater reserves. *Journal of Hydrology* 373:122–138

542 Graham LP, Hagemann S, Jaun S, Beniston M (2007) On interpreting hydrological change from
543 regional climate models. *Climatic Change* 81:97–122

544 Grindley J (1967) The estimation of soil moisture deficits. *Meteorological Magazine* 96:97–108

545 Guardiola-Albert C, Murillo JM, Martín Machuca M, Mediavilla C, López Geta JA (2005) Modelo
546 matemático revisado del acuífero Almonte-Marismas, aplicación a distintas hipótesis de gestión.

547 Proceedings of the VI Symposium of Water in Andalusia II: 799–810

548 Guardiola-Albert C, García-Bravo N, Mediavilla C, Martín Machuca M (2009) Gestión de los
549 recursos hídricos subterráneos en el entorno de Doñana con el apoyo del modelo matemático del
550 acuífero Almonte-Marismas. *Boletín Geológico y Minero*, 120: 361–376

551 Hughes AG, Mansour MM and Robins NS (2008) Evaluation of distributed recharge in an upland
552 semi-arid karst system: the West Bank Mountain Aquifer, Middle East. *Hydrogeology Journal*
553 16:845–854

554 IGME (1992) Hidrogeología del Parque Nacional de Doñana y su entorno. Colección informes de
555 aguas subterráneas y geotecnia, Technical Report of Spanish Geological Survey. Madrid

556 IGME (2009) Mejora del modelo matemático del acuífero Almonte-Marismas como apoyo a la
557 gestión de los recursos hídricos: estimación de la recarga, modelo estocástico y
558 actualización. Technical Report of Spanish Geological Survey. Madrid

559 IPCC (2000) Special report on emissions scenarios. Summary for policymakers. Cambridge
560 University Press, United Kingdom

561 IPCC (2007) Climate change 2007: The physical science basis. Contribution of Working Group I to
562 the Fourth Assessment Report of the Intergovernmental Panel on Climate Change, Cambridge,
563 United Kingdom

564 Jackson, CR., Meister R, Prudhomme C (2011). Modelling the effects of climate change and its
565 uncertainty on UK Chalk groundwater resources from an ensemble of global climate model
566 projections. *Journal of Hydrology*. 399:12–28

567 Junta de Andalucía (2009) II Plan de Desarrollo Sostenible. Doñana. Memoria Informativa.
568 Consejería de Medio Ambiente, 87p. [http://www.pds.donana.es/documentos_publicos/
569 1257323614359.pdf](http://www.pds.donana.es/documentos_publicos/1257323614359.pdf). Accessed 2 Sep 2010

570 Kilsby CG, Jones PD, Burton A, Ford AC, Fowler HJ, Harpham C, James P, Smith A, Wilby RL
571 (2007) A daily weather generator for use in climate change studies. *Environmental Modelling &
572 Software* 22:1705–1719

573 Kuhn NJ, Baumhauer R, Schütt B (2011) Managing the impact of climate change on the hydrology
574 of the Gallocante Basin, NE-Spain. *Journal of Environmental Management* 92: 275–283

575 Lerner D, Issar SA, Simmers I (1990) Groundwater recharge. Verlag Heinz Heise

576 McDonald MG, Harbaugh AW (1988) A modular three-dimensional finite-difference ground-water
577 flow model: U.S. Geological Survey Techniques of Water-Resources Investigations, book 6,
578 chap. A1

579 Mansour MM, Hughes AG (2004) User's manual for the distributed recharge model ZOODRM.
580 British Geological Survey Internal Report IR/04/150

581 Manzano M, Custodio E, Cardoso da Silva G, Lambán J (1998) Modelación del efecto del cambio
582 climático sobre la recarga en dos acuíferos carbonatados del área mediterránea. 4º Congreso
583 Latinoamericano de Hidrología Subterránea, Montevideo, Uruguay. ALHSUD 1:322–333

584 Penman HL (1948) Natural evaporation from open water, bare soil and grass, Proceedings of the
585 Royal Society of London, Series A, 193:120–145

586 Primack AGB (2000) Simulation of climate-change effects on riparian vegetation in the Per
587 Marquette River, Michiga. Wetlands 20:538–547

588 Prudic DE, Konikow LF, Banta ER (2004) A new stream-flow routing (SFR1) package to simulate
589 stream-aquifer interaction with MODFLOW-2000: U.S. Geological Survey Open-File Report
590 2004-1042

591 Rodríguez-Rodríguez M, Benabente J, Cruz-San Julián JJ, Moral Martos F (2006) Estimation of
592 ground-water exchange with semi-arid playa lakes (Antequera region, southern Spain). Journal
593 of Arid Environments 66:272–289

594 Segui PQ, Ribes A, Martín E, Habets F, Boe J. (2010). Comparison of three downscaling methods
595 in simulating the impact of climate change on the hydrology of Mediterranean basins. Journal of
596 Hydrology 383:111–124

597 Serrano L, Reina M, Martín G, Reyes I, Arechederra A, León D, Toja J (2006) The aquatic systems
598 of Doñana (SW Spain): watersheds and frontiers. Limnetica 25:11–32

599 Sousa A, García Murillo P (1999) Historical evolution of the Abalarío lagoon complexes (Doñana
600 Natural Park, SW Spain). Limnetica 16:85–98

601 Sousa A, García Murillo P (2003) Changes in wetlands of Andalusia (Doñana Natural Park, SW
602 Spain) at the end of the little Ice Age. *Climate Change* 58:193–217

603 Trick T, Custodio E (2004) Hydrodynamic characteristics of the western Doñana Region (area of El
604 Abalarío), Huelva, Spain. *Hydrogeology Journal* 12:321–335

605 UPC (1999) Modelo regional de flujo subterráneo del sistema acuífero Almonte-Marismas y su
606 entorno. Technical Report of the Technical University of Catalonia, Barcelona

607 Wilby RL, Wigley TML, Conway D, Jones D, Hewitson BC, Main J, Wilks DS (1998) Statistical
608 downscaling of general circulation model output: a comparison of methods. *Water Resources*
609 *Research* 34:2995–3008

610 Wilby RL, Harris I (2006). A framework for assessing uncertainties in climate change impacts:
611 Low-flow scenarios for the River Thames, UK. *Water Resources Research*.
612 Doi:10.1029/2005WR004065

613 Younger PL, Teutsh G, Custodio E, Elliot T, Manzano M, Satuer M (2002) Assessments of the
614 sensitivity to climate change of flow and natural water quality in four major carbonate aquifers
615 of Europe. *Sustainable groundwater development* In: Hiscock KM, Rivett MO, Davison RM
616 (eds). *Geological Society Special Publication* 193:303–323

617 Woldeamlak ST, Batelaan O, De Smedt F (2007) Effects of climate change on the groundwater
618 system in the Grote-Nete catchment, Belgium. *Hydrogeology Journal* 15:891–901

619 WWF España (2006) Doñana y Cambio Climático.
620 http://assets.wwfes.panda.org/downloads/informe_wwf_donana_cambio_climatico1_2006.pdf.
621 Accessed 2 Sep 2010

Model	IPCC-DDC	Modelling Group	Country	Spatial Resolution
	Acronym			Mesh (Long x Lat)
CNRM-CM3	CNCM3	Météo-France / Centre National de Recherches Météorologiques	France	Gaussian 128 x 64
CSIRO-Mk3.0	CSMK3	CSIRO Atmospheric Research	Australia	Gaussian 192 x 96
ECHO-G	ECHOG	Meteorological Institute of the University of Bonn, KMA meteorological inst., and M & D group	Germany / Korea	Gaussian 96 x 48
GFDL-CM2.0	GFCM20	Geophysical Fluid Dynamics Laboratory	USA	Regular 144 x 90
GFDL-CM2.1	GFCM21	Geophysical Fluid Dynamics Laboratory	USA	Regular 144 x 90
GISS-ER	GIER	NASA / Goddard Institute for Space Studies	USA	Regular 72 x 46
UKMO-HADCM3	HADCM3	UK Met Office	UK	Regular 96 x 73
INM-CM3.0	INCM3	Institute for Numerical Mathematics	Russia	Regular 72 x 45
IPSL-CM4	IPCM4	Institut Pierre Simon Laplace	France	Regular 96 x 72
MIROC3.2 (medres)	MIMR	National Institute for Environmental Studies, and Frontier Research Centre for Global Change	Japan	Gaussian 128 x 64
ECHAM5/MPI-OM	MPEH5	Max Planck Institute for Meteorology	Germany	Gaussian 192 x 96
CCSM3	NCCCSM	National Centre for Atmospheric Research	USA	Gaussian 256 x 128
PCM	NCPCM	National Centre for Atmospheric Research	USA	Gaussian 128 x 64

623 Table 1 GCMs considered in this study. More details at <http://www-pcmdi.llnl.gov>

Month	1	2	3	4	5	6	7	8	9	10	11	12
Los Palacios y Villafranca ET ₀ (mm day ⁻¹)	1.4	2	2.9	4.2	5.3	6.2	6.4	5.7	4.3	2.7	1.7	1.2
Blaney Criddle ET ₀ (mm day ⁻¹)	1.4	2.1	2.9	4.3	5.3	6.1	6.2	5.6	4.2	2.6	1.7	1.3
Los Palacios y Villafranca temperature (°C)	10.2	11.5	13.9	15.2	18.1	21.2	23.9	23.5	21.7	18.4	13.9	11.2
Precipitation San Lucar de Barrameda (mm day ⁻¹)	2.48	2.45	0.98	1.22	1	0.3	0.03	0.09	0.66	1.81	2.86	3.45

625 Table 2 Monthly mean values of (i) measured reference evaporation ET₀ (mm day⁻¹) at Los Palacios
626 y Villafranca meteorological station for the period October 2000 to March 2007, (ii) calculated
627 reference evaporation ET₀ (mm day⁻¹) using the Blaney Criddle method, (iii) temperature (°C) at
628 Los Palacios y Villafranca meteorological station for the period November 1978 to March 2007,
629 and (iv) precipitation at Sanlucar Barrameda 'INM' meteorological station for the period 1975 to
630 1997

631

Simulation	ME (m)	MAE (m)	SRMSE (%)
Steady-state	0.23	4.45	4.05
1975-1997	-0.04	3.33	2.88

632 Table 3 Head error measures: mean error (ME), mean absolute error (MAE) and standard root mean
633 square error (SRMSE).

634

	La Rocina basin	El Partido basin	Las Marismas basin	Guadamar basin
Mean historic (1975-1997) groundwater discharge to basin	33.8	11.3	39.4	8.4
Mean historic groundwater abstraction for irrigation	7.8	0.3	18.2	0.1
Mean historic groundwater abstraction for public supply	0.2	0	0.4	0
Simulated change in groundwater discharge to basin due to climate change	Maximum	-18.7	-8.3	-26.7
	Ensemble average	-12.2	-1.7	-20.7
	Minimum	-8.4	+0.4	-16.9

635 Table 4. Comparison of historic groundwater abstraction and simulated decreases in groundwater
636 discharge to stream basins under future climate (hm³/year)

637

638 **Figures**

639 **Fig. 1** (a) Location of Almonte-Marismas aquifer. (b) Surface geology. (c) Two schematic
640 geological cross-sections based on IGME (1992) and Custodio et al. (2009)

641 **Fig. 2** Groundwater model structure and boundary conditions

642 **Fig. 3** Observed and simulated groundwater levels at selected observation boreholes

643 **Fig. 4** Projected changes in precipitation, temperature and PE for the 2080s under the A2 emissions
644 scenario for the GCMs listed in Table 1

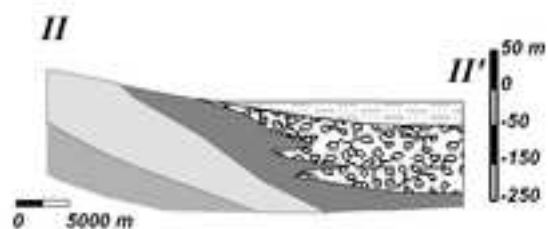
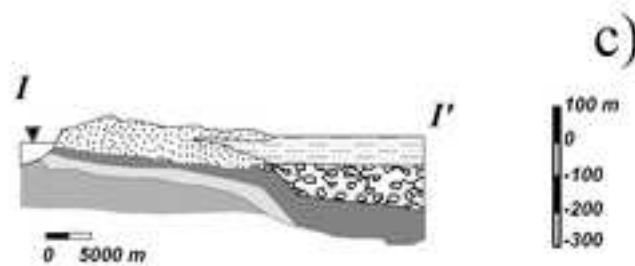
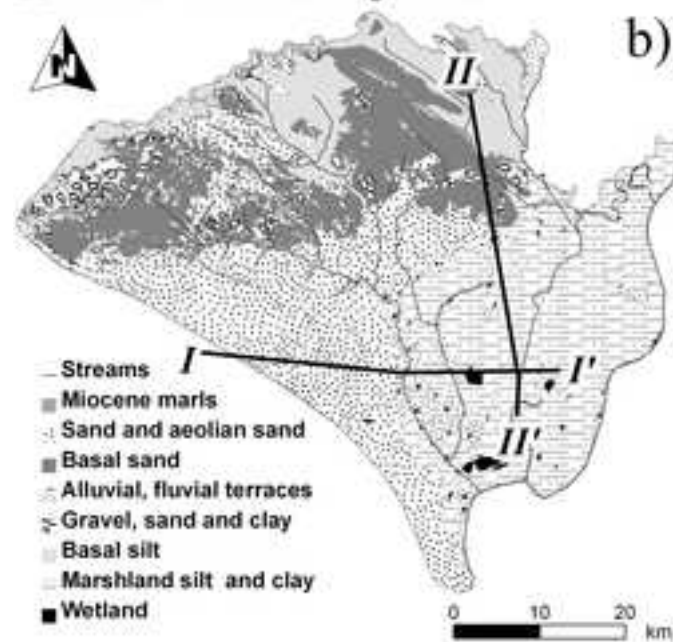
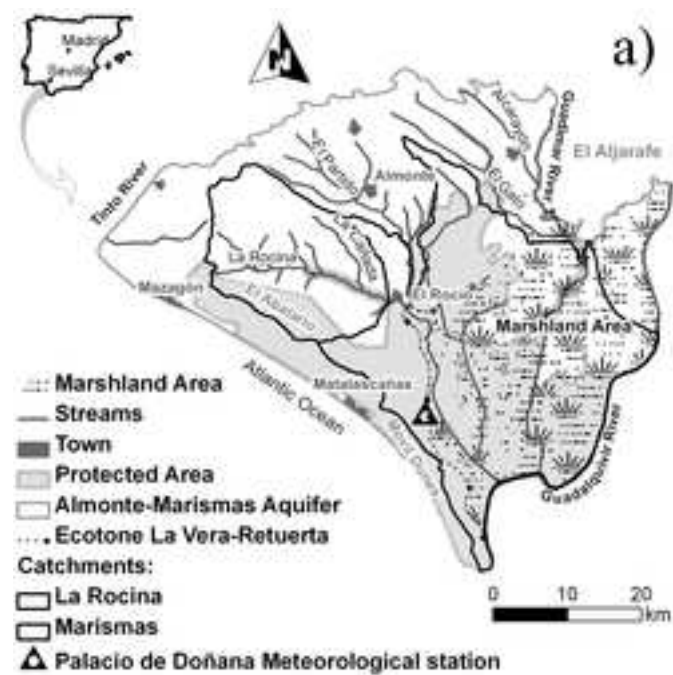
645 **Fig. 5** Simulated monthly mean recharge for the baseline (1975–1997) and 2080s time-slices under
646 the A2 emissions scenario

647 **Fig. 6** Differences in groundwater levels across the aquifer for December 2084 relative to the
648 December 1979 in the baseline period. Values were reclassified to range from 2 to -17 m

649 **Fig. 7** Simulated monthly mean flows to the sea for the baseline (1975–1997) and 2080s time-slices
650 under the A2 emissions scenario

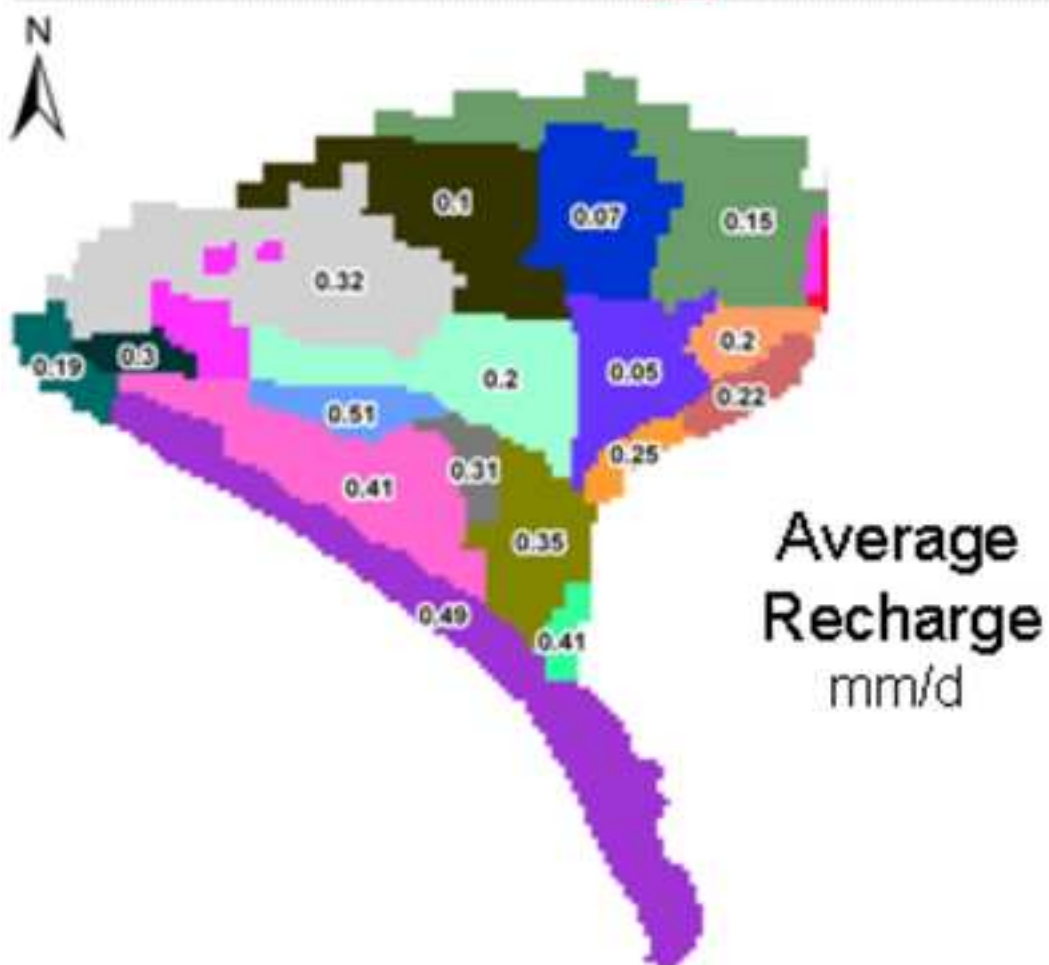
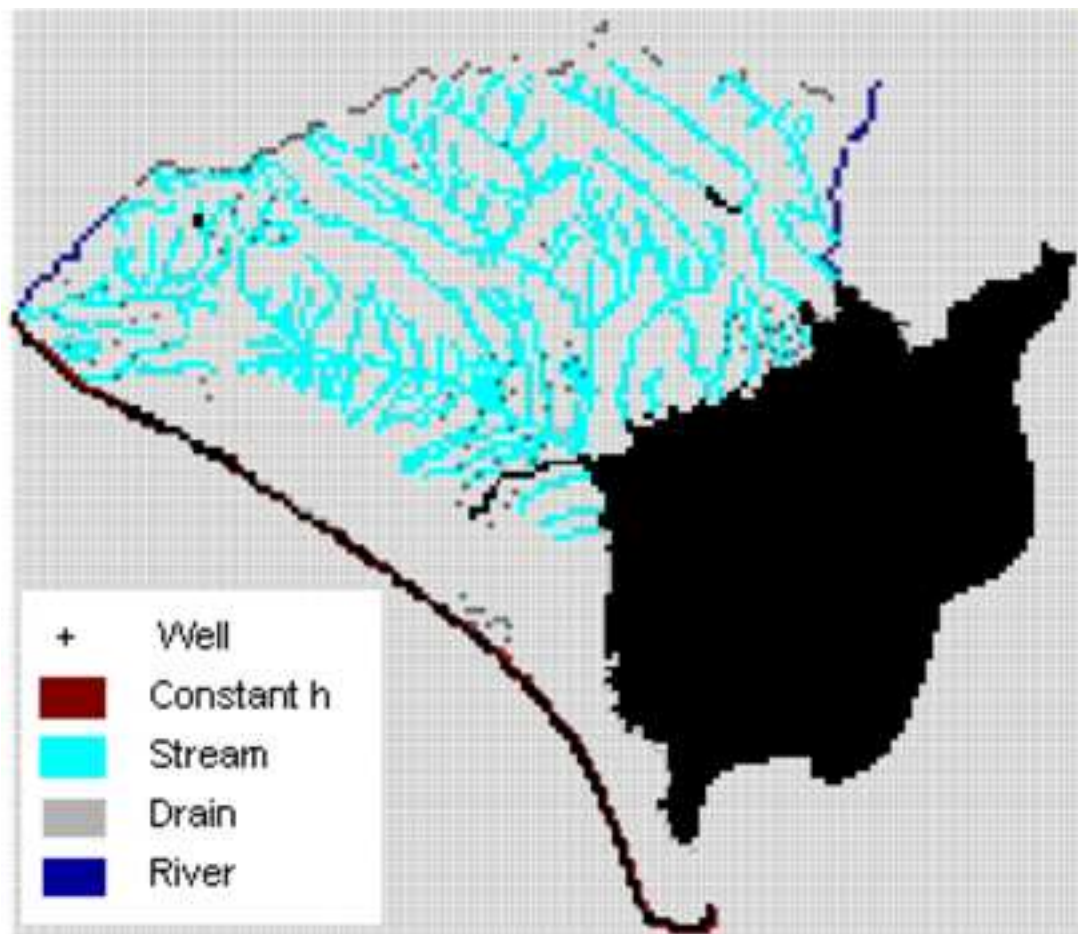
colour figure

[Click here to download high resolution image](#)

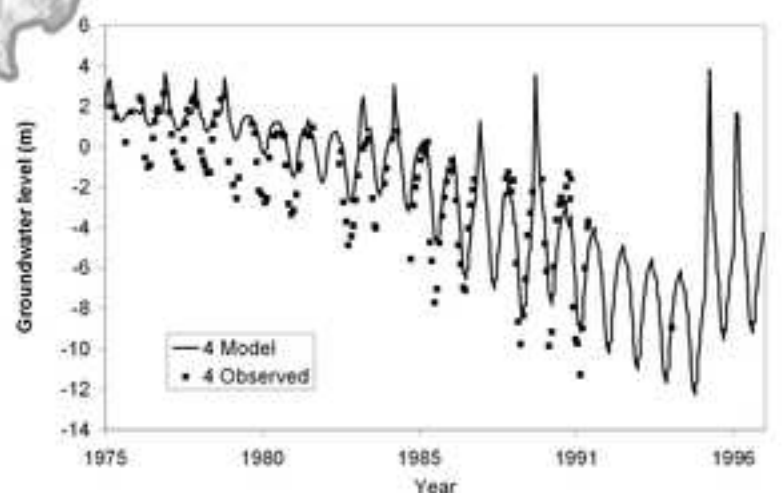
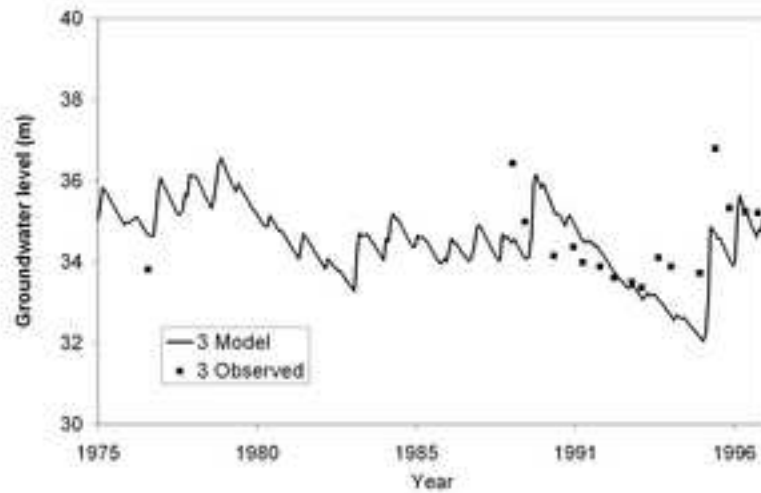
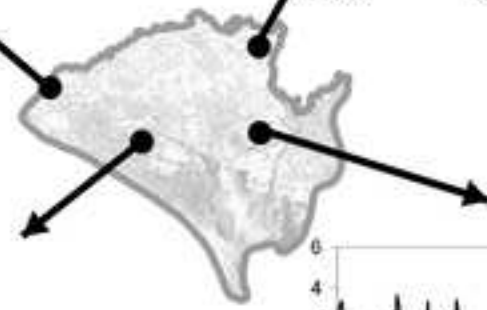
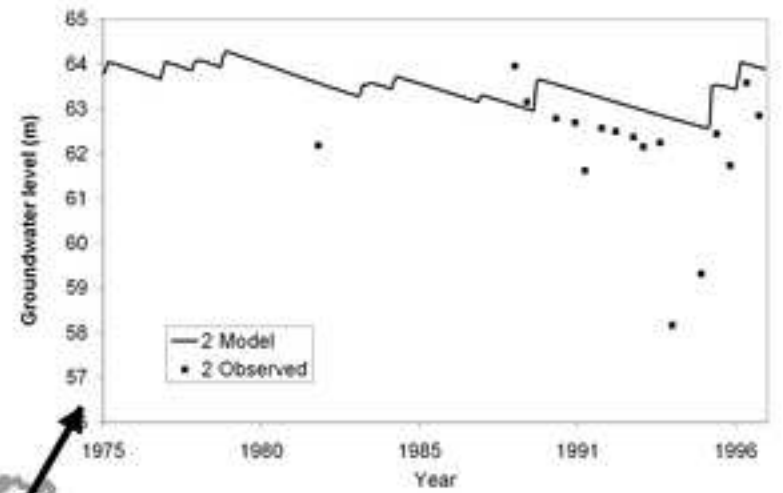
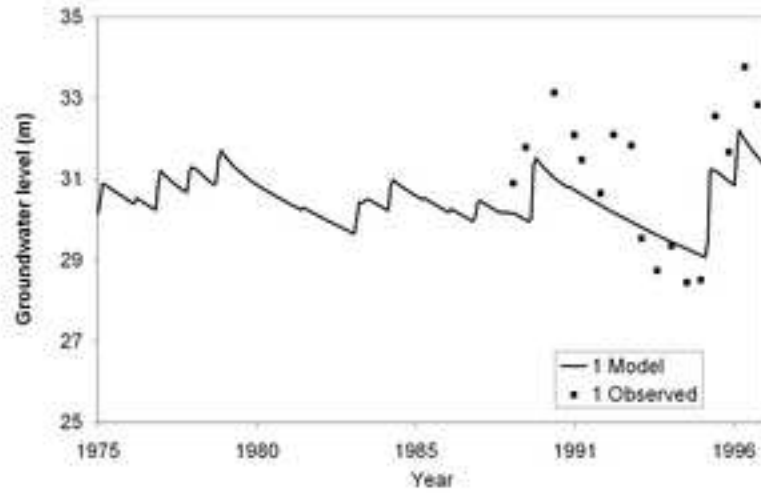


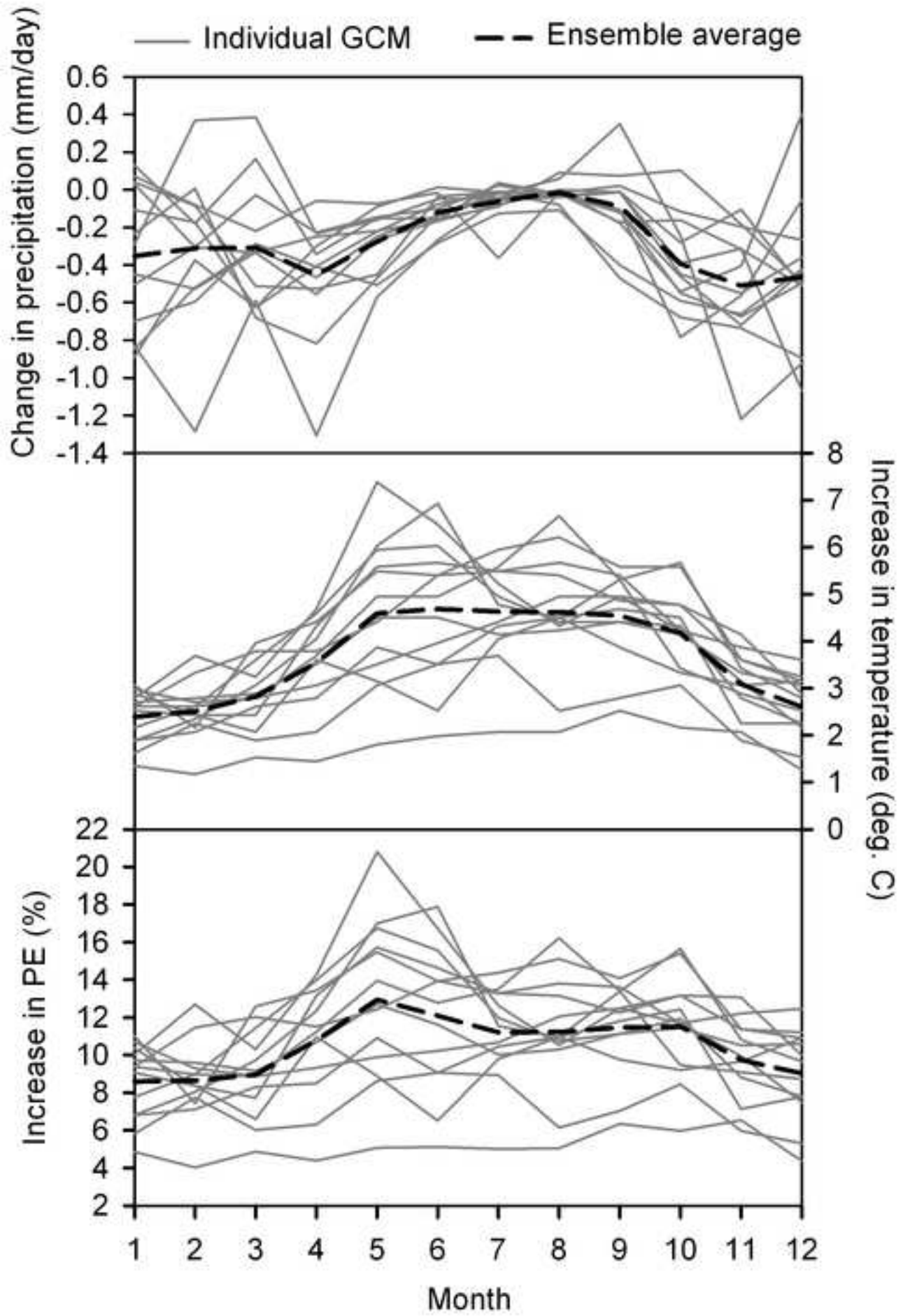
colour figure

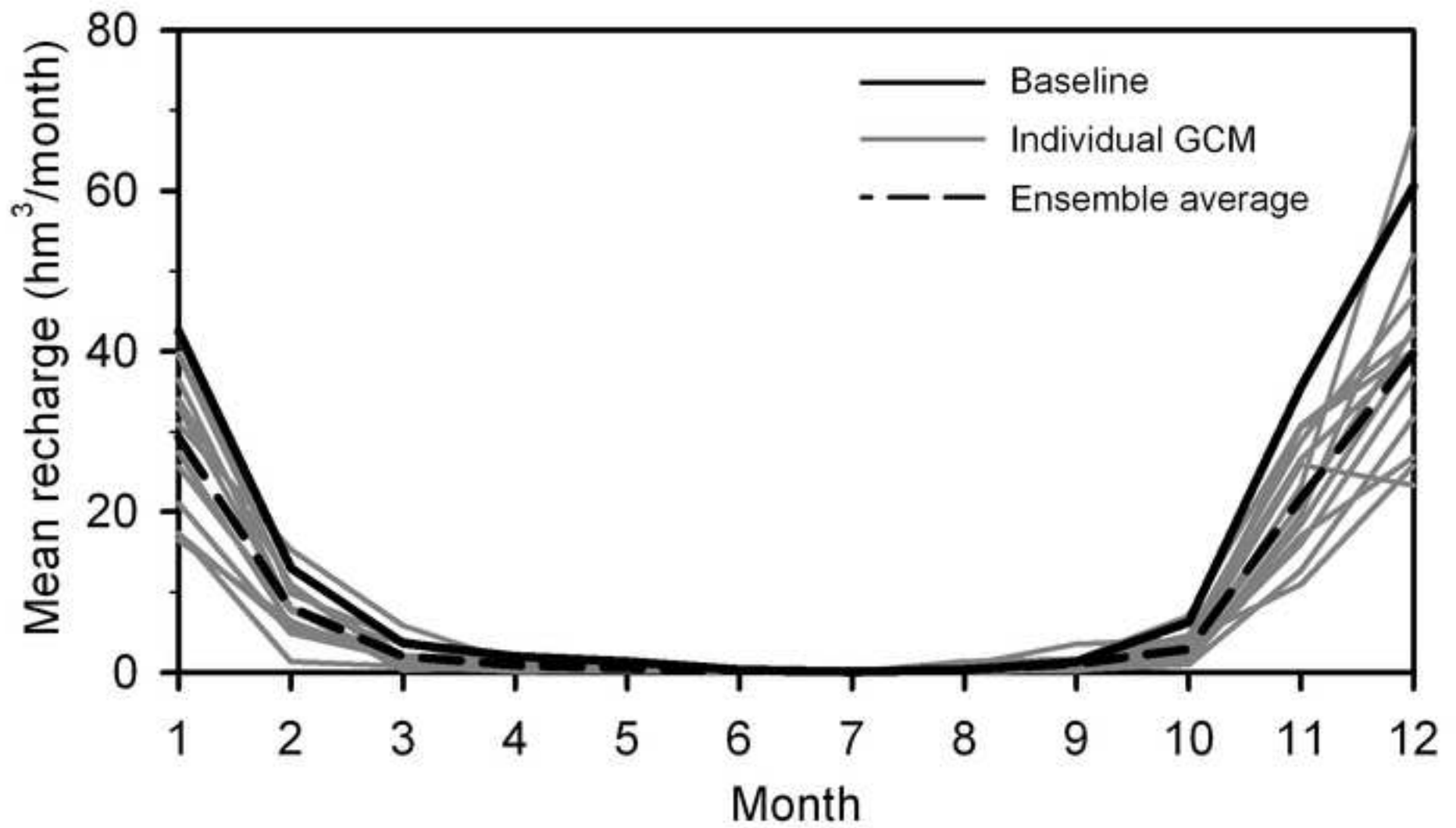
[Click here to download high resolution image](#)



colour figure
[Click here to download high resolution image](#)







Groundwater level differences in December 2084 relative to December 1979

